BREAKING THE RULES: INCREASED INVASIVE AGGRESSION IN CHEMO-RESISTANT LYMPHOMA

An Honors Fellows Thesis

by

EVAN MICHAEL CHERRY

Submitted to the Honors Programs Office
Texas A&M University
in partial fulfillment of the requirements for the designation as

HONORS UNDERGRADUATE RESEARCH FELLOW

April 2010

Major: Chemical Engineering

BREAKING THE RULES: INCREASED INVASIVE AGGRESSION IN CHEMO-RESISTANT LYMPHOMA

An Honors Fellows Thesis

by

EVAN MICHAEL CHERRY

Submitted to the Honors Programs Office
Texas A&M University
in partial fulfillment of the requirements for the designation as

HONORS UNDERGRADUATE RESEARCH FELLOW

Approved by:

Co-Research Advisors:	Kayla Bayless
	Steve Maxwell
Associate Director of the Honors Programs Office:	Dave A. Louis

April 2010

Major: Chemical Engineering

ABSTRACT

Breaking the Rules: Increased Invasive Aggression in Chemo-Resistant Lymphoma.
(April 2010)

Evan Michael Cherry
Department of Chemical Engineering
Texas A&M University

Research Advisors: Dr. Kayla Bayless, Dr. Steve Maxwell
Department of Molecular & Cellular Medicine

Diffuse Large B Cell Lymphoma (DLBCL) is a common form of cancer, accounting for 30% of all lymphoma diagnoses. Patient survival rates of DLBCL are roughly 30-40% with the standard chemotherapeutic cocktail consisting of cyclophosphamide, doxorubicin, vincristine, and prednisone (CHOP therapy). Approximately 50% of patients develop chemoresistance to CHOP therapy and succumb to metastasis of vital organs. To penetrate tissues and organs, lymphoma cells must invade the extracellular matrix surrounding blood vessels. We investigated the ability of CHOP-resistant lymphoma to invade three-dimensional collagen matrices mimicking the extracellular matrix. We evaluated the potential for cellular dyes to quantify invasion responses and developed a protocol for automated fluorescent quantification of invasion responses. Further, because the cytoskeleton is critical for cell locomotion and morphology, we investigated the role of key cytoskeletal proteins vimentin, actin, and tubulin in lymphoma invasion. Our data indicate that microtubule stabilization, but not

depolymerization, inhibits CHOP-resistant lymphoma invasion. Additionally, depolymerization of actin and vimentin completely blocked invasion responses. Altogether, this work develops a quantifiable model to study lymphoma invasion, mimic metastasis, understand cytoskeletal function, and gain further insight into molecular signals required for cellular invasion in three-dimensional matrices.

ACKNOWLEDGMENTS

Thanks to Dr. Bayless for a wonderful opportunity and training experience, and for all her guidance, patience, understanding, and encouragement.

Thanks to Dr. Maxwell for generating the cell lines, providing insight into cancer biology, and collaborating on this project.

Thanks to Dr. Louis and the Honors Programs Office for counseling, Undergraduate Research Fellows Funding, and Summer University Undergraduate Research Funding.

Special thanks to Dr. Warren Zimmer and Josephine Hernandez for a wonderful experience with the Texas A&M Health Science Center 2009 Summer Undergraduate Research Program.

Special thanks to Dr. Sacchettini for suggesting the use of alamar blue and providing us with initial samples.

Special thanks to Dr. Alaniz and Jane Miller for instructions on how to sterile sort the cells by flow cytometry.

Special thanks to the Bayless lab: Adriana, Vaidehi, Henry, Shih-Chi, and Hojin for help and support.

NOMENCLATURE

AB	Alamar Blue (Resazurin)
bFGF	Basic Fibroblast Growth Factor
CHOP	Cyclophosphamide, Hydroxydaunorubicin, Oncovin, and Prednisone
CT488	Celltrace Oregon Green 488
DiI	1,1'-dioctadecyl-3,3,3'3'-tetramethylindocarbocyanine perchlorate
DLBCL	Diffuse Large B Cell Lymphoma
EGF	Epidermal Growth Factor
FACS	Fluorescence-Activated Cell Sorting
FBS	Fetal Bovine Serum
GFP	Green Fluorescent Protein
HPLC	High-Performance Liquid Chromatography
IGF	Insulin-like Growth Factor
LPA	Lysophosphatidic Acid
MMP	Matrix Metalloproteinase
MTT	Dimethyl thiazolyl diphenyl tetrazolium
PBS	Phosphate-Buffered Saline
K	Thousand
RFU	Relative Fluorescence Unit

RPMI	Roswell Park Memorial Institute Medium 1640
S1P	Sphingosine-1-Phosphate
UV	Ultraviolet
VEGF	Vascular Endothelial Growth Factor

TABLE OF CONTENTS

Page

LIST OF FIGURES

LIST OF TABLES

CHAPTER I

INTRODUCTION

Diffuse large B cell lymphoma and non-Hodgkins lymphoma

Lymphoma is a type of cancer that originates in the immune system due to malignant lymphocytes. Lymphocytes such as T and B cells are types of white blood cells that mediate the active immune response. Lymphoma was first discovered and characterized by Thomas Hodgkin, a british physician, who noticed tumor growth in lymph tissue [1].

Non-Hodgkins Lymphoma is a class of lymphoma encompassing strains other than those described by Thomas Hodgkin in 1832 [2]. Classes of Lymphoma are divided based on lymphocyte origin as well as cell size and shape. Lymphoma classes can be further divided into subclasses based on specific genetic irregularities that cause lymphoma. Diffuse Large B Cell Lymphoma (DLBCL) is a very aggressive strain of non-Hodgkins lymphoma, caused by malignant B cells. DLBCL is the most prevalent strain of non-Hodgkins Lymphoma, accounting for more than 30% of all diagnoses.

CHOP and chemotherapy resistance

Metastasis occurs due to the accumulation and invasion of cancer cells into nearby

---

This thesis follows the style of *Biophysical and Biochemical Research Communications*.

tissues, ultimately leading to patient mortality. To combat malignant cells chemotherapeutic agents target rapidly dividing cells. One major strategy is to disrupt the cells' ability to rearrange their cytoskeleton, arrest the cell in a non-metabolic period, prevent the cell from dividing, and kill the cell [3]. However, cancerous cells eventually become chemo-resistant, even to high-dose regimens [4]. These mechanisms of chemo-resistance require new treatments for preventing the spread and proliferation of cancer cells.

CHOP, a combination of Cyclophosphamide, Hydroxydaunorubicin (Doxorubicin), Oncovin (Vincristine), and Prednisone, is the standard strategy for treating DLBCL because it is as effective as and less toxic than other chemotherapy regimens [5-6]. The survival rate of non-Hodgkins Lymphoma with CHOP therapy is roughly 30-40%, but when the patient becomes CHOP-resistant, the survival rate plummets [7].

Cellular invasion

Cellular invasion is an otherwise normal physiological process, applicable to wound healing, angiogenesis (blood vessel formation), and the immune response. In the immune response, signaling lipids such as lysophosphatidic acid (LPA) and sphingosine-1-phosphate (S1P) encourage lymphocyte proliferation and migration [8-10]. Additionally, signaling peptides (mitogens) called growth Factors (GFs) are usually required to activate proteins that signal for cell motility [11].

The most visible aspect of cellular motility and invasion is morphology changes due to reorganization of the cytoskeleton, roughly analogous to muscle and bone movement in higher organisms. Specifically, three types of cytoskeletal elements are important to cell shape and motility: microtubules, microfilaments, and intermediate filaments [12]. Cell morphology change is a dynamic process in the invasion response, as we have demonstrated with endothelial cells in (Fig. 1) [13].

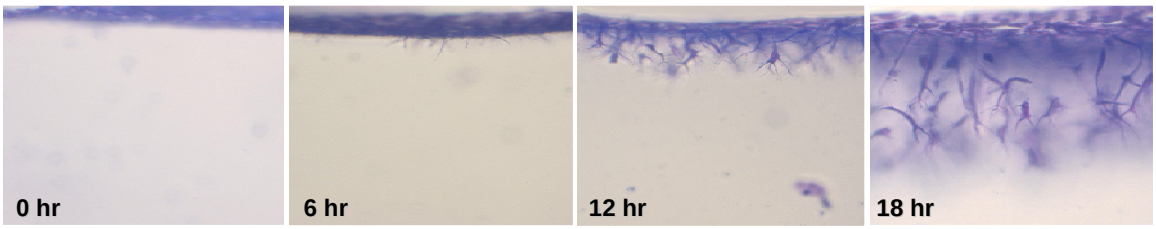

Fig. 1**.** Endothelial cells invade 3-dimensional collagen matrices.

The cytoskeletal protein tubulin is the target for many therapies, including treatment for cancer and gout. Physiological levels for cytoskeletal drugs vincristine (Fig. 2A), colchicine (Fig. 2B), and paclitaxel (Fig. 2C) have been determined from HPLC [14-16] and will be used at these concentrations in our enclosed studies on drug-resistant parent cell lines generated previously in the laboratory [17].

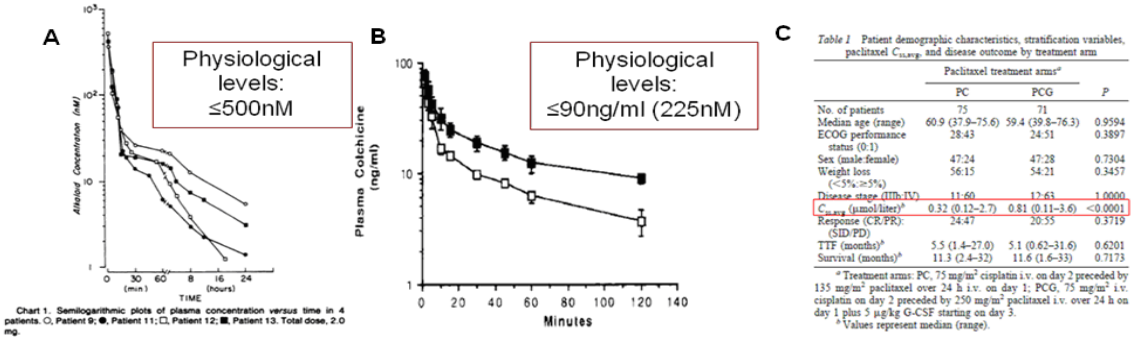

Fig. 2**.** Cytoskeletal drugs vincristine (A), colchicine (B), and paclitaxel (C).

CHAPTER II

METHODS

Reagents

All reagents were from Sigma-Aldrich (St. Louis, MO) unless otherwise stated.

Collagen extraction

Rat tail collagen type I was isolated by soaking frozen rat tails in ethanol, removing the epidermis from the tails, extracting tendons, and removing any muscle or fatty tissue. Tendons were then soaked in 150 ml of sterile 0.1% (vol/vol) acetic acid and gently shaken for 48 hours. Every 24 hours thereafter the solution was centrifuged and 40 ml extracts were removed from the supernatant and added to separate tubes. Extracts were combined in a lyophilizer bottle and rotated while shell-freezing in dry ice until all liquid was frozen. Frozen solution was lyophilized until dry product was white and fibrous. Dry collagen product was weighed and dissolved overnight in 0.1% acetic acid to a final solution of 7.1mg collagen/ml.

Isolation of CHOP-resistant DLBCL cell lines

Diffuse large B cell lymphoma line CRL2631 was obtained from the American Type Culture Collection. Cells were propagated in RPMI 1640 supplemented with 2 mM L-glutamine, 1.5 g/L sodium bicarbonate, 4.5 g/L glucose, 10 mM HEPES, 1.0 mM sodium pyruvate, and 10% fetal bovine serum. Cells were passaged every 2 to 3 days to

maintain a density between 1-2 x 10^6 cells/ml. Four to five T75 flasks each containing a total of 3 x 10^7 DLBCL cells in 30 ml of medium (1 x 10^6 cells/ml) were treated with on-off cycles of CHOP exposure. The composition of CHOP consisted of cyclophosphamide, doxorubicin, vincristine, and prednisone at the clinical ratio of 80/5.5/0.16/11.1, respectively, with the highest combined CHOP concentration set at 1280 ng/ml and the lowest at 5 ng/ml. Cyclophosphamide and doxorubicin were dissolved in Millipore-purified water, vincristine was dissolved in methanol, and prednisone was dissolved in chloroform/ethanol (1:1). CHOP reagents were stored at -80^{o}C. Similar to patient CHOP regimens, cells were subjected to cycles of 5 day CHOP treatment followed by 21 days of recovery in the absence of CHOP. Cells were initially selected with several cycles of 80 ng/ml CHOP. After several on-off cycles in 80 ng/ml CHOP, viable cells were treated with several on-off cycles of a higher CHOP dose (160 ng/ml). Cycling with CHOP was continued until a cell population emerged that could survive and recover from 5-day exposures to 640 ng/ml CHOP. Three independently derived CHOP-resistant populations (designated G1, G2, G3) were derived from the CRL2631 cell line. Cell line G2 was used for this project.

Cell culture

Lymphoma cultures were grown in 5-10 ml of RPMI 1640 (RPMI) containing 10% FBS (Cambrex), 0.01 mg/ml Gentamycin Reagent Solution (Invitrogen), 1X MEM Non-essential Amino Acids (Invitrogen), 1mM Sodium Pyruvate (Invitrogen), and 1X Antibiotic-Antimycotic (Invitrogen) in 25 cm^2 flasks (Corning Incorporated). 3-5 ml of

cell suspension were aspirated and replaced with fresh medium every 3-4 days. For invasion experiments, cells were counted with a hemacytometer, centrifuged, and resuspended in RPMI to $1x10^5$ cells/50 µl unless otherwise indicated.

Vertical collagen invasion assay

1 mg/ml collagen matrices were prepared by combining 350 µl of 7.1 mg/ml collagen type I solution, 39 µl 10X M199, 2.1 µl 5N NaOH, and 2109 µl RPMI, keeping gel on ice and mixing thoroughly after adding each component. 28 µl of gel was added to wells in a 96-well plate (Corning Inc.) and allowed to polymerize and equilibrate at 37°C and 5% CO_2 for 10 min. G2 cells (100,000 cells/50 µl/well) were added to the wells and allowed to adhere. After seeding the cells, each well was given 50 µl of RPMI containing reduced-serum II supplement and the indicated concentrations of test compounds. Cells were allowed to invade for 48h before fluorescent staining. After quantification, cells were fixed in 3% glutaraldehyde in PBS and stained with 0.1% toluidine blue in 30% methanol before being counted using an eyepiece with an ocular grid. Three fields at the center of each triplicate were selected and counted manually at the specified magnification. Data is presented as invading cells per field (±SD). For cross-sectional photographs, gels were scored with a needle, placed on a microscope slide, cut into cross-sectional slices, and placed sideways. Pictures were taken and analyzed using an Olympus SC35 Type 12S Digital Camera and QCapture Pro Software (QImaging Co.).

Automated quantification

At the end of 48h invasion, the culture media from the 96-well plate was tossed and the plate was submerged in sterile saline at 37^{o}C and shaken vigorously/tossed 5-10 times. The saline was then tossed and each well was treated with indicated cellular label. 0.1% toluidine blue and 1.09 μM DAPI were added for 20 minutes and 24 hours, respectively, after fixing the cells for 20 minutes in 3% glutaraldehyde in PBS. Cells stained in 100 μl of RPMI with 20 μM DiI, 2 μM Celltrace Oregon Green 488 (Invitrogen), and 20μg/ml Texas Red-conjugated *Lycopersicon esculentum* (Tomato) Lectin (Vector Laboratories) were rotated at 37^{o}C for 1h before reading. Cells stained with 20 μg/ml Alamar Blue (resazurin) were incubated at 37^{o}C for 8-24h with special care to read the plate before all dye was metabolized. Fluorescence or absorbance was read using a Bio-TEK Synergy HT Plate reader and KC4 software. Absorbance, excitation, and emission wavelength settings are summarized in Table 1**.**

Table 1. Absorbance and fluorescence settings for cellular dyes.

Dye	Absorbance (nm)	Excitation (nm)	Emission (nm)
Toluidine Blue	562		
DAPI		360/40	460/40
DiI		530/25	590/20
TR-Lectin		590/20	645/40
CT488		485/20	528/20
GFP		485/20	528/20
Alamar Blue	595	530/25	590/20

Generation of G2-GFP

293FT cells were grown on 20 μg/ml collagen in DMEM with 10% FBS to full confluence. 293FT were transfected with lentiviral backbone and helper plasmids expressing GFP and blasticidin resistance for 8 hours. Viral particles were harvested after 72 h and combined 50:50 with RPMI with 10% FBS and 12 μg/ml polybrene. G2 cells were treated with viral media for 48 h. GFP expression was verified by observing emission of green light when excited with 480nm UV light. Stable transfected cells were selected with blasticidin and sterile sorted by flow cytometry using a FACSAria II. The final population expressed greater than 9000 FITC-A units and reflected the 3.8% brightest GFP-expressing cells from the stable culture.

Cytoskeletal altering compounds

Microtubules were depolymerized using 1μM solutions of vincristine sulfate (Oncovin®) and vinblastine sulfate. To verify that the effects of vincristine and vinblastine on invasion were not due to drug resistance, cells were treated with 200nM of the non-vinca alkaloid microtubule depolymerizing agent colchicine. Microtubules were stabilized with 1 μM paclitaxel (Taxol®). Actin and vimentin were depolymerized using 1 μM cytochalasin D and 1 μM withaferin A (EMD Biosciences), respectively.

CHAPTER III

RESULTS

We initially tested the invasion response of two lymphoma cell lines: CHOP-sensitive 2631 and a CHOP-resistant progeny G3 [17]. Our initial experiments revealed that CHOP-resistant cells were notably more invasive than the CHOP-resistant parent line (Fig. 3A). Furthermore, the lymphoma cells are invading by changing their morphology to penetrate the gel (Fig. 3B). Through manually counting the number of invading cells, we determined that the average number of invading G3 cells was increased over the average number of invading 2631 cells by a factor of 4.3 (Fig. 3C).

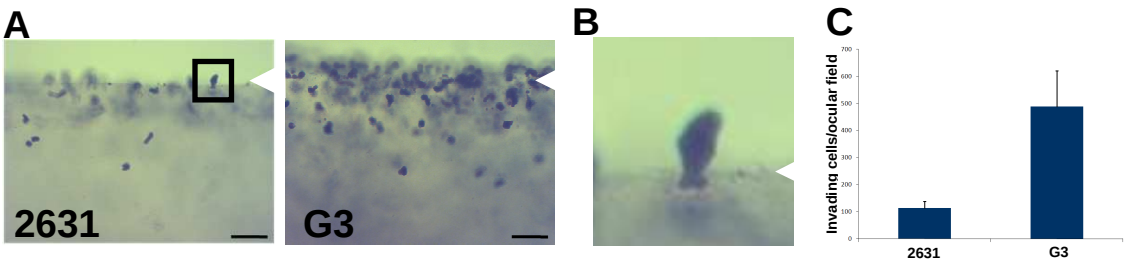

Fig. 3. CHOP-resistant cells are more invasive. Cross-sectional views of CHOP-sensitive 2631 and CHOP-resistant G3 invasion in 3-dimensional collagen matrices (A) with a magnified view of an invading cell (B) and manual quantification of the average number of invading cells (C). White arrows indicate original cell monolayer. Bar=50 μm.

We next optimized the number of invading cells and the duration of the experiment using another CHOP-resistant line derived from 2631 named G2. We decided to use G2 because its metabolism is slightly slower than G3 and G2 survives longer in the assay without requiring change in medium (data not shown). G2 cells invade over the course

of 48 h, with the majority of invasion occurring after 24 h (Fig. 4A). The number of cells seeded on the gel at the beginning of the experiment was varied to determine if cell confluence was required for invasion (Fig. 4B). However, at 48 h there were cells navigating the gel, revealing that the cells are inherently invasive. Optimal conditions were determined by comparing all cell numbers over the course of 48 h (Fig. 4C).

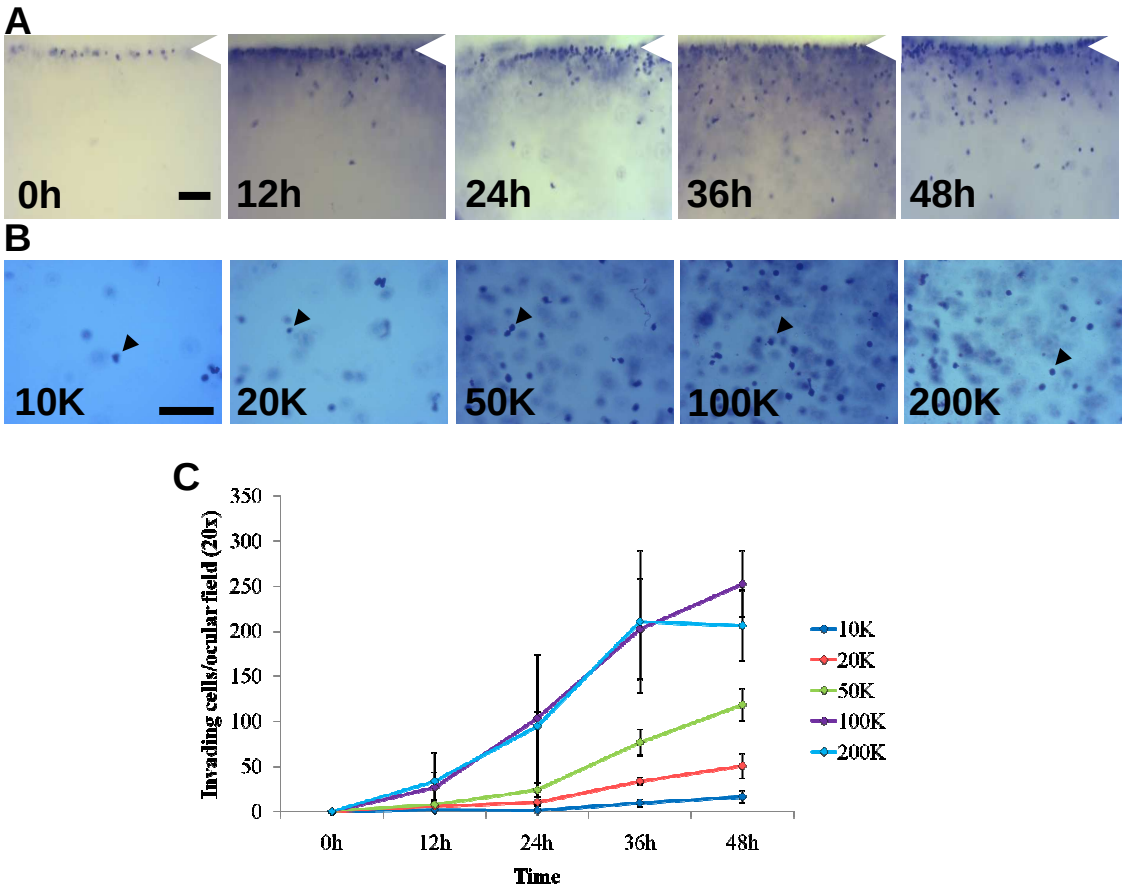

Fig. 4. G2 invasion assay optimization. (A) Cross-sectional views of invading G2 over 48 h and (B) top views of various numbers of invading cells on the monolayer are summarized (C) for 10-200K cells over 48 h (C). White arrows indicate original cell monolayer and black arrows indicate invading cells. Bar=100 μm.

For the greatest sensitivity, we wanted to select the conditions that resulted in the greatest number of invading cells. While both 100K and 200K seeded cells followed

similar invasion responses for the first 36 h, 100K had the greatest number of invading cells at 48 h. The decrease in invasion for 200K at 48 h is likely due to overconsumption of nutrients or accumulation of metabolic waste. Subsequent experiments were conducted by seeding 100K cells and allowing 48 h for invasion.

To determine a suitable fluorescent compound for quantification, we investigated several cellular dyes and markers (Fig. 5A). We selected a membrane stain (toluidine blue), a fluorescent membrane stain (DiI), a fluorescent nuclear stain (DAPI), a fluorescent-conjugated analogue of tomato lectin, a fluorescent cytosolic protein marker (CT488) and a metabolic dye resazurin (Alamar Blue ®).

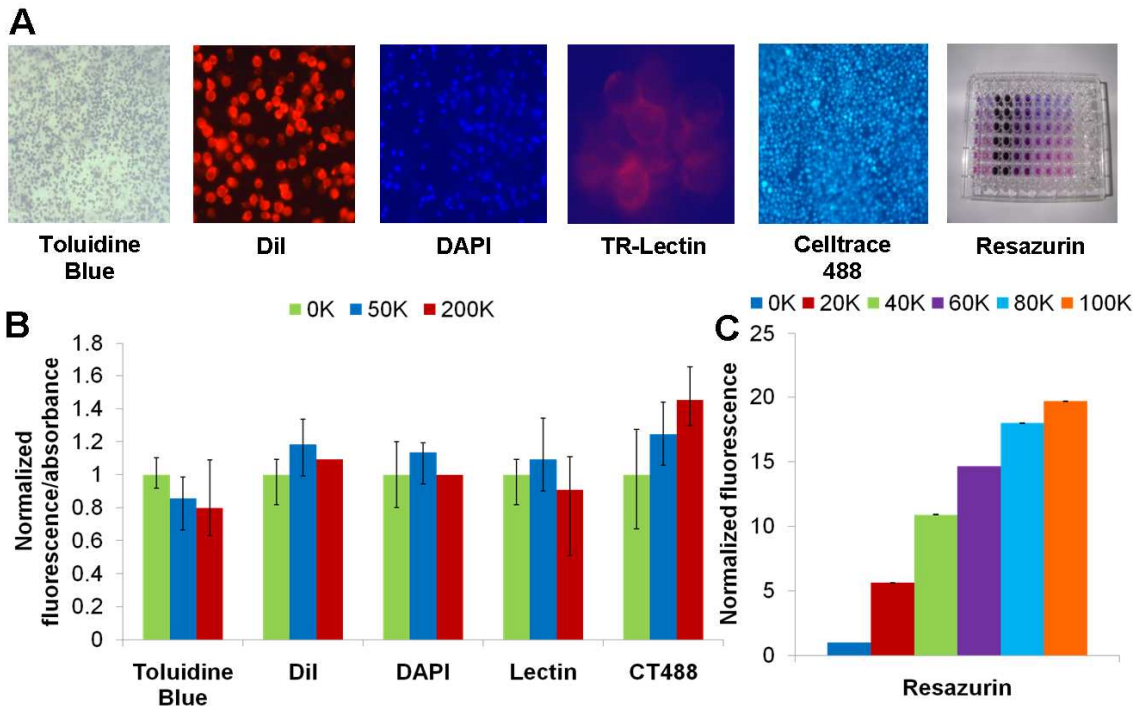

Fig. 5. Quantification of G2 invasion with various cellular dyes. (A)Various cellular dyes tested and (B) normalized quantification for 0K, 50K, and 200K cells in collagen gels. (C) Resazurin sensitivity for a 0K-100K cell curve.

Initial experiments for each dye tested their ability to accurately detect cell numbers and differentiate between 0, 50K, and 200K cells already present in the gel (Fig. 5B). Initial experiments determined that labeling the cells before placing them on the gels inhibited invasion and was not ideal for studying metastasis (data not shown). Ideally, increasing cell numbers should demonstrate increased signal without significant overlap. Toluidine blue absorbance was not a good candidate due to high variability and low sensitivity. DiI and lectin were unable to permeate the gel and stain the cells after the invasion assay (data not shown), resulting in minimal changes in fluorescent signal with increasing cell numbers. DAPI fluorescence was indistinguishable by the plate reader. CT488 demonstrated the correct signal trends; however, there was significant overlap in signal indicating high variability and insufficient sensitivity. Resazurin showed considerable sensitivity for smaller differences in cell numbers (Fig. 5C) without significant overlap, making it a prime candidate for automated quantification.

After investigating fluorescent cell markers, we transfected G2 with GFP, a benign fluorescent protein. After transfecting and establishing a stable culture resistant to blasticidin, we sorted cells based on their level of GFP expression by fluorescence-activated cell sorting (FACS) using a FACS-Aria II (Fig. 6A). We sorted and collected the 3.8% brightest GFP-expressing cells and photographed cells under phase (Fig. 6B) and UV light (Fig. 6C).

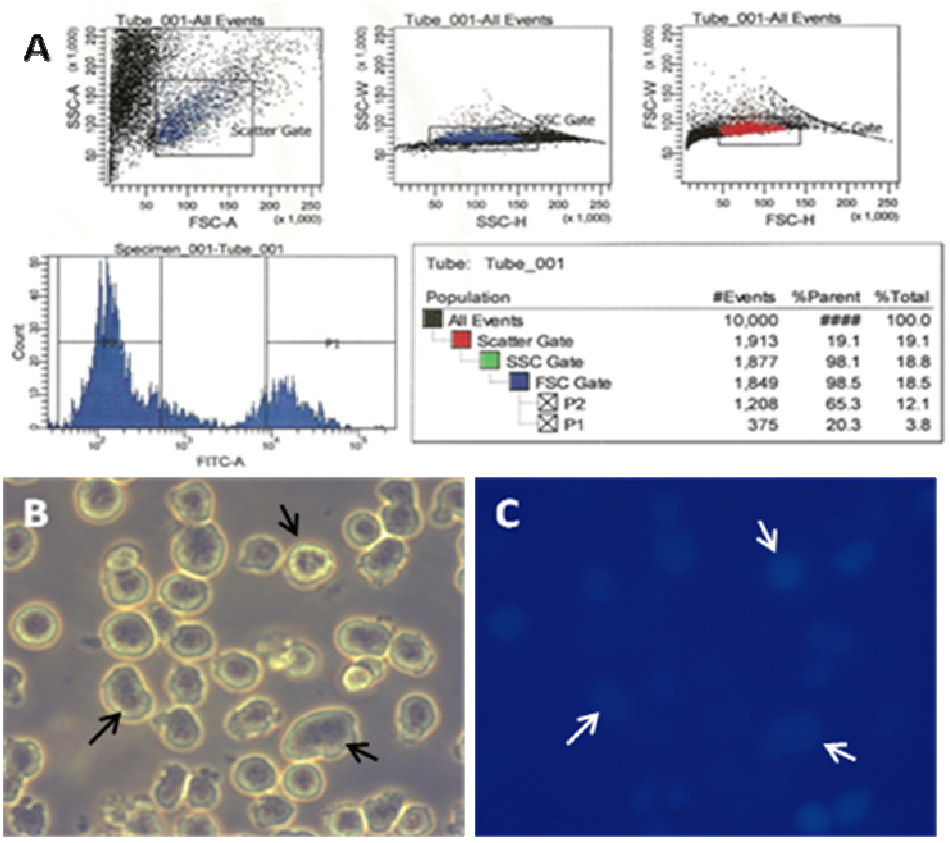

Fig. 6. Isolation of G2-GFP. Stable GFP-expressing G2 were (A) isolated with a FACS-Aria II and compared under (B) phase and (C) UV light. Arrows indicate the same cell visible under normal light and GFP fluorescence.

Despite successful isolation of GFP-positive cells, invasion experiments with the G2-GFP cells demonstrated that the GFP signal was not intense enough to register on the platereader (data not shown).

Based on encouraging results from the fluorescent metabolic dye resazurin (Alamar Blue®), we decided to optimize conditions to quantify invasion. From our previous dye experiments, we determined that initial experiments should determine the ability of the dye to permeate the collagen gel and reflect cell numbers. After verifying the ability of

Alamar Blue to penetrate the gel, we conducted experiments to optimize resazurin concentration for 0-100K cells already present in the gel (Fig 7A).

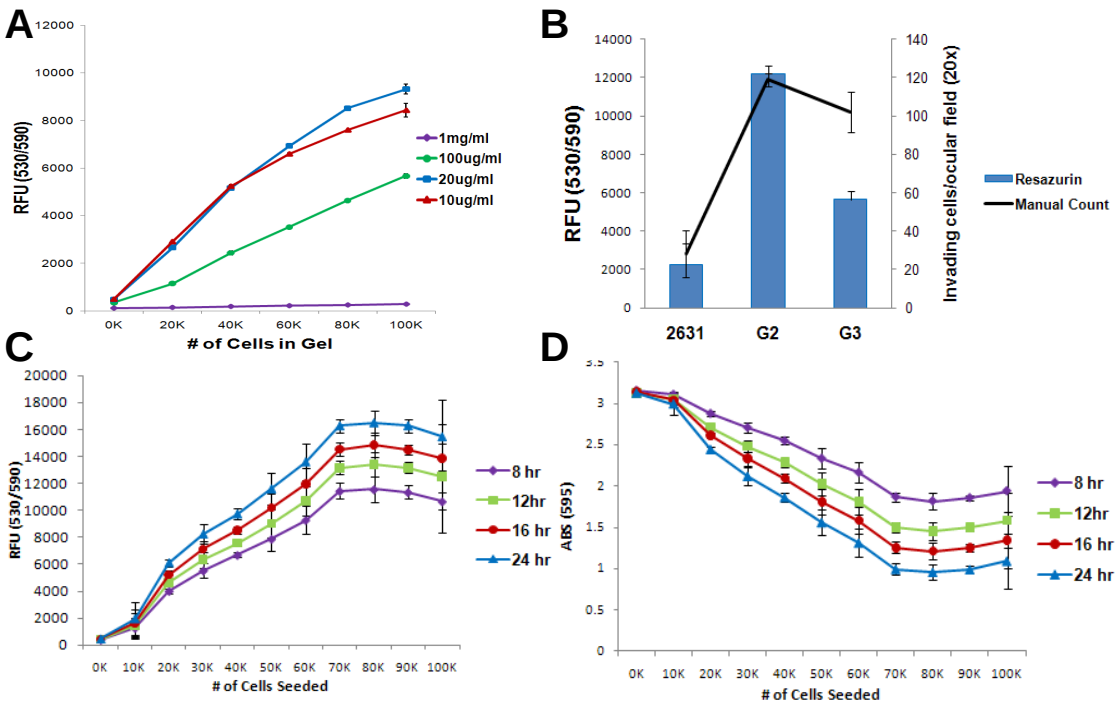

Fig. 7. Optimization of resazurin quantification. Resazurin incubation was (A) optimized for concentration and (B) compared with a manual count to verify accurate reflection of invasion for 2631, G2, and G3. (C) Fluorescence and (D) absorbance were analyzed with a platereader for a resazurin incubation time course for varying numbers of seeded cells.

To maximize sensitivity for differences in fluorescence, we selected 20 µg/ml as the working concentration. 1 mg/ml and 100 µg/ml were deemed too toxic and 10 µg/ml did not produce the strongest signal for differences between 80K and 100K seeded cells. To verify the accuracy of our model, we compared a manual count of 2631, G2, and G3 to fluorescence data from an overnight incubation with 20 µg/ml resazurin (Fig. 7B). The trend was accurately reflected for all three cell types, although the relative fluorescence-invasion agreement for G3 was not as sensitive as agreement for 2631 and G2. We

conducted a time course for resazurin incubation for a cell curve of 0-100K seeded cells to optimize the number of seeded cells and resazurin incubation time and determine whether quantification via fluorescence (Fig. 7C) or absorbance (Fig. 7D) was more sensitive. The trend along the cell curve was consistent for both quantification via fluorescence and absorbance between 8 and 24 hours of incubation (absorbance readings are inverse of fluorescence readings). Interestingly, the dye becomes saturated when processed by 70K or more cells, indicating that there is no benefit to seeding more than 70K cells under normal conditions. Beyond 24 hours, small differences in the number of invading cells are lost due to dye saturation; therefore, the ideal window for quantification is between 8 and 24 hours. We determined 16 hours as the most convenient incubation period because resazurin can be added in the afternoon, incubated overnight, and read on the platereader the next morning.

After optimizing the invasion assay, we investigated the effects of various cytoskeletal inhibitors on G2 invasion. Using physiological doses, we added paclitaxel, vincristine, vinblastine, colchicine, withaferin A, and cytochalasin D to invading cells after seeding them on the gel. From manual quantification of invading cells (Fig. 8A) and cross-sectional photographs of the wells (Fig. 8B), we discovered that microtubule depolymerization with vincristine (1μM), vinblastine (1μM), and colchicine (200nM) did not inhibit invasion, whereas microtubule stabilization with paclitaxel significantly inhibited invasion ($p=0.006$) at a physiological dose. Vincristine treatment increased invasion ($p=0.038$).

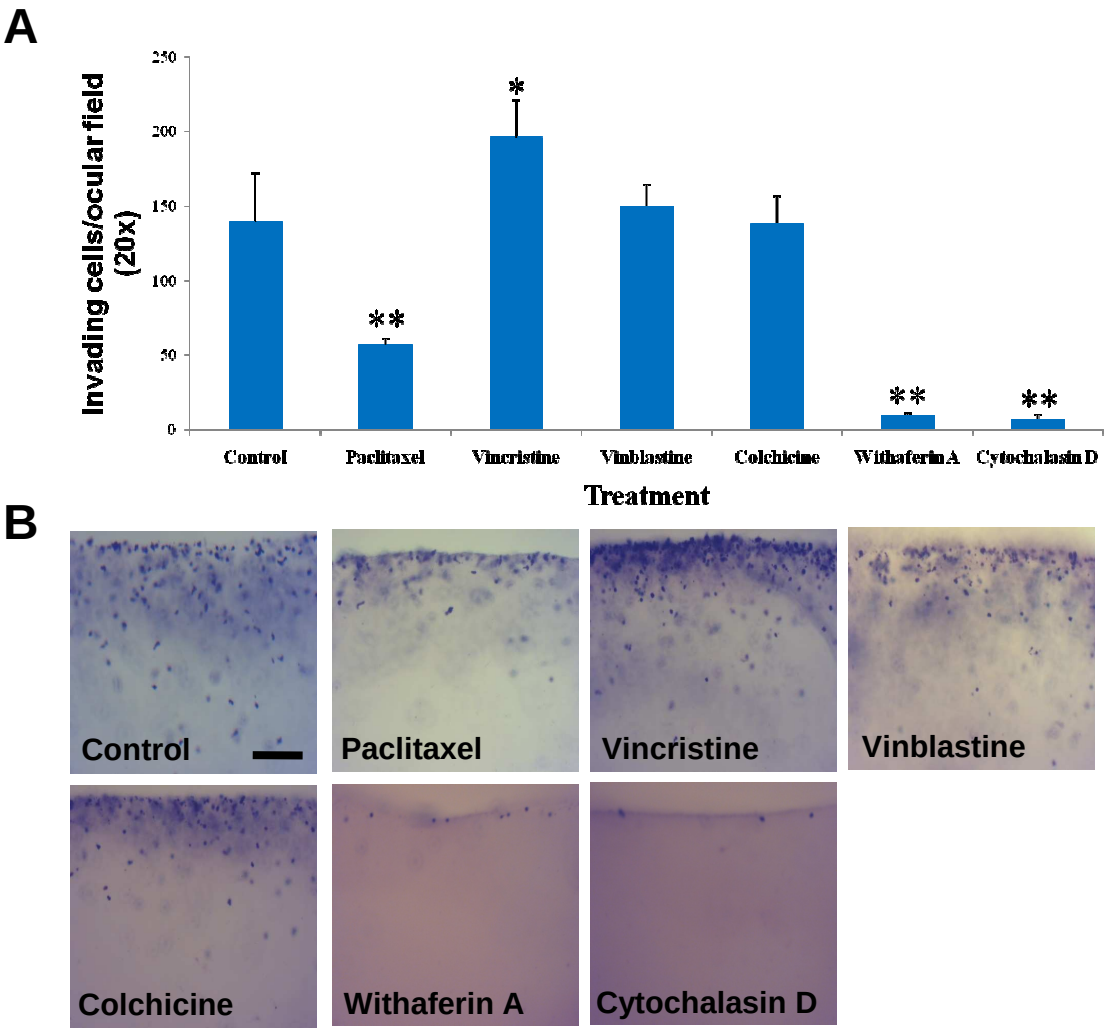

Fig. 8. Effects of cytoskeletal drugs on G2 invasion. (A) Manual quantification and (B) cross-sectional photographs of invading cells treated with cytoskeletal drugs . All drug concentrations were 1μM except for 200 nM colchicine. * represents a p-value of <0.05, ** represents a p-value of <0.01 vs. control. Bar=200 μm.

Withaferin A, a vimentin depolymerizing agent, and Cytochalasin D, an actin depolymerizing agent, both nearly completely inhibited invasion at a concentration of 1μM (p=0.001).

We tested the ability of resazurin to accurately quantify the number of invading cells by comparing resazurin data to a manual count for a withaferin dose response (Fig 9).

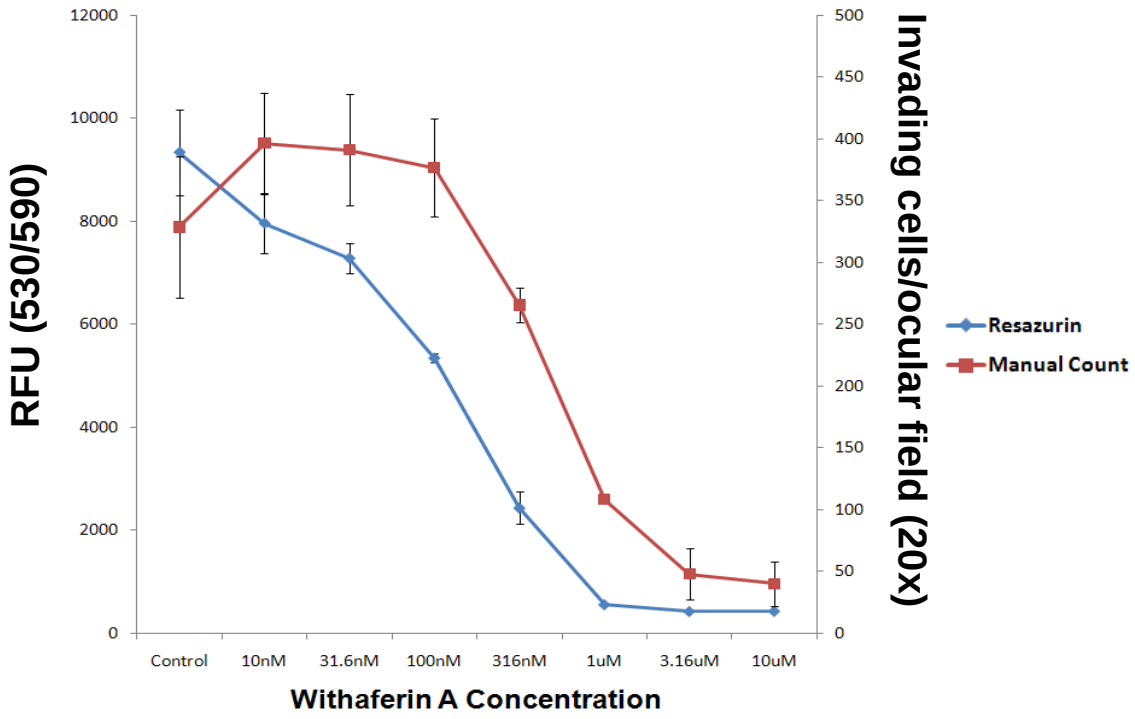

Fig. 9. Manual and objective quantification of a withaferin dose curve. A semi-logarithmic curve of G2 invasion in the presence of withaferin A was quantified by manual counting and resazurin quantification.

The trends both show a dose-dependent decrease in invasion with increasing withaferin A concentration; resazurin sensitivity is apparent between 31.6nM and 100nM, where a slight decrease in cells correlated to a significant difference in resazurin signal. Additionally, both data sets display flat endpoints above the effective blocking dose of 1μM.

To better understand the nature of lymphoma invasion, we tested the effects of the pro-proliferation and pro-motility cytokines LPA and S1P in the collagen matrix in the presence and absence of a growth factor (GF) mixture of vascular endothelial growth factor (VEGF), basic fibroblast growth factor (bFGF), epidermal growth factor (EGF), and insulin-like growth factor (IGF). We quantified this experiment with our resazurin protocol (Fig. 10).

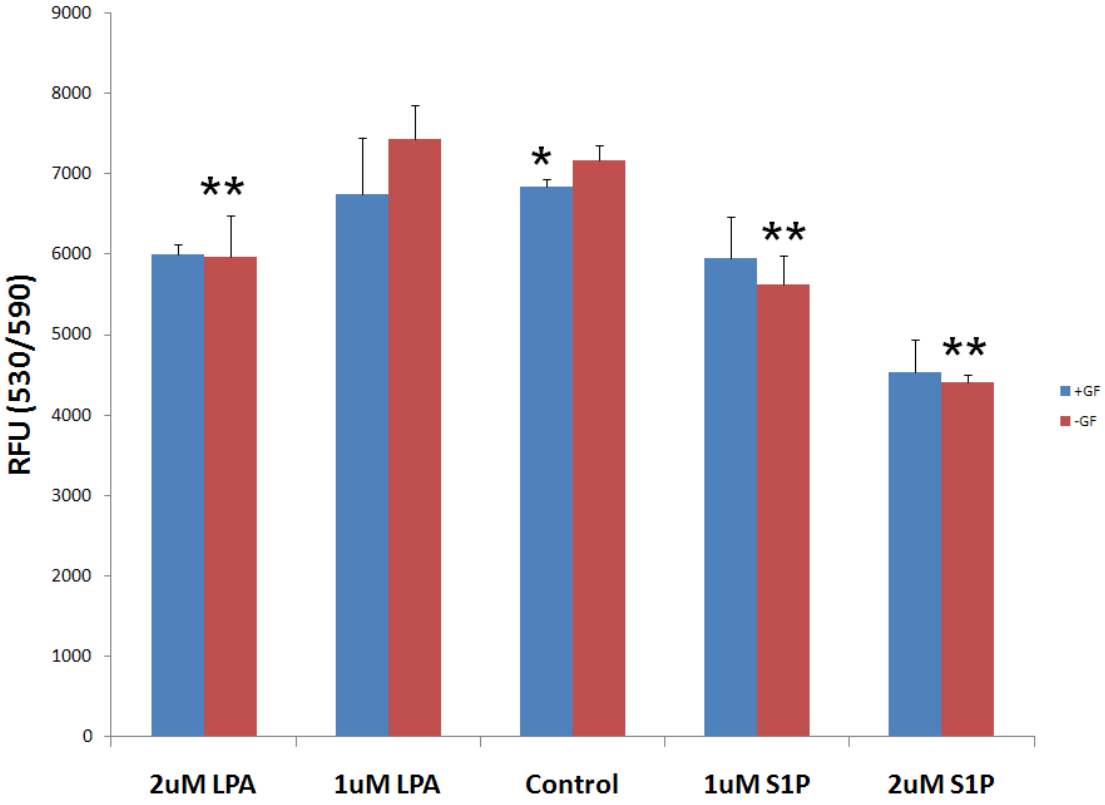

Fig. 10. Effects of growth factors, LPA, and S1P on G2 invasion. LPA and S1P were added to the gel before cells were seeded with or without growth factors. * represents a p-value of <0.05 vs. GF. ** represents a p-value of <0.01 vs. control without GF.

According to these data, the GF mixture had a slight negative, if not negligible, effect on lymphoma invasion. 2μM LPA, 1uM S1P, and 2μM S1P inhibited invasion.

CHAPTER IV

SUMMARY AND DISCUSSION

Summary

We have designed a lymphoma invasion assay that is objectively quantifiable through the use of the cellular dye resazurin; optimal resazurin quantification occurs with 70,000 seeded cells/well treated with 20ug/ml resazurin for 12-16h. Altogether, this assay provides a quantifiable model for lymphoma invasion into 3-dimensional collagen matrices mimicking the extracellular matrix. To invade, CHOP-resistant lymphoma cells require dynamic tubulin instability and intact vimentin and actin polymers, possibly due to a shift in cytoskeletal organization to accommodate the loss of microtubules associated with chemotherapy. CHOP-resistant lymphoma are inherently more aggressive and does not require growth factors, LPA, and S1P, which are cytokines that typically promote cell motility. Applications include metastatic potential, proteomic and biochemical analyses, drug screening, and pharmacological studies.

Discussion

Previous viability assays, such as MTT [18] and MTS [19] assays, are limited to colorimetric assays and require additional steps to solubilize the reductase product. Our assay removes this requirement and utilizes a one-time addition of resazurin in media and the option of quantification by absorbance or fluorescence. With this resazurin method, variability due to intermediate solvent additions to solubilize the product and their effects on cellular metabolism are avoided. Alamar blue assays have been

established for determining cell growth and survival of cancer cells [20] and for determining cellular viability after screening with potential drugs [21]. Our assay integrates the detection of viable invading cells into an invasion assay, allowing for rapid and objective high-throughput screening of potential anti-metastatic drugs and selective targeting of factors related to CHOP-resistance.

The cytoskeletal composition of cells is similar to that of a macroorganism. Microtublules are large structures that provide the majority of structure and serve as anchors for smaller cytoskeletal proteins similar to a skeletal system. Vimentin acts as a weaker but more flexible structure akin to cartilage and its role in cellular signaling may parallel the nervous system. Actomyosin structures are analogous to cellular muscles and are responsible for the contractile physiology of muscle tissue. The results for the various cytoskeletal drugs are understandable in this context: an organism must be able to physically move itself and have the proper support and signaling for effective movement. Successful actin and vimentin polymerization would therefore be required to pull the invading cell through the extracellular matrix. As evidenced by invertebrates, bones are not a universal necessity. Excessive microtubule stabilization and polymerization caused by paclitaxel is likely due to limited flexibility; too many bones, hyperostosis, causes the organism to become too rigid and impairs mobility.

Separate studies uncovered a noticeable up-regulation of multiple proteins controlling motility in the CHOP-resistant lines and prompted our lab to test whether drug-resistant

lines were more invasive in 3-dimensional collagen matrices. Vimentin expression increases in endothelial cells during angiogenesis [22] and correlates with a period of increased cellular motility. High levels of vimentin expression are associated with increased metastasis and a poor prognosis in breast cancer [23], particularly for cancer cells resistant to microtubule depolymerizing/DNA intercalating agents [24]. Vimentin up-regulation has also been identified as a factor for increased motility in prostate cell cancer cells [25]. The exact role of vimentin in cellular motility is still unclear, but some research suggests that vimentin mediates matrix adhesion [26]. We theorize that cancer cells up-regulate vimentin to accommodate the loss of microtubules associated with CHOP therapy. Vimentin fibrils can move rapidly without changing overall cell shape [27], a desirable characteristic for more motile cells as they scramble to accommodate invasive structures. Conversely, because assembly of vimentin networks is dependent on microtubule-associated kinesins [28], loss of microtubule integrity would result in ineffective regulation of vimentin polymerization.

Microtubule depolymerization can induce cellular motility [29] and activate Rho-dependent pathways [30]. Rho-family protein expression has been used as biomarker for cancer cells[31-32] and shown to mediate the organization of the actin cytoskeleton , enhance motility, and promote degradation of the extracellular matrix[33]. Resistance to multiple microtubule depolymerizing agents has been shown to be occur in Chinese hamster ovarian cells[34] after treatment with a single agent, indicating the possibility that repeated microtubule depolymerization causes a shift in normal dependence on

microtubules. Because vincristine is a principle component of CHOP, our data raise the possibility that repeated therapy likely contributes to the increased invasion in our resistant cell lines. It is therefore imperative to investigate other targets for treating lymphoma or discovering compounds that selectively target resistant cell lines. Using the method developed here, we can begin to study these events.

As the smallest and most transient cytoskeletal element, actin localization at the membrane is essential for the formation of local invadopodia/podosome structures required for metastasis [35-36]. In our experiments, actin depolymerization with cytochalasin D greatly inhibited the ability for G2 to invade. As evidenced by (Fig. 3B), lymphoma are invading by extending portions of the membrane and "stepping" into the matrix. Targeting the proteins required for actin localization at the membrane would likely be an effective therapy for metastatic cancer.

S1P and LPA increase cellular motility for some types of cancer[37-38], but we have not discovered any positive effect of LPA or S1P for lymphoma invasion. S1P and LPA insensitivity have been linked to metastatic cancer [39] and S1P/LPA receptors are being investigated as treatment for metastatic cancer [40]. LPA has also been identified as an indirect inhibitor of matrix metalloproteinases (MMPs) [41], enzymes required for digesting the extracellular matrix. MMPs are required for endothelial cell migration [42-43], but their role in lymphoma metastasis is unclear. MMP localization at the membrane and extracellular matrix digestion at the membrane are linked to podosomes and

metastasis [44] and Rho-mediated pathways [37]. Long-standing debates theories of amoeboid movement continue [45] and several groups doubt the ability for cells to navigate the extracellular matrix without degradation [46-47]. We plan to conduct invasion experiments with various MMP inhibitors, analyze them using our protocol, and investigate the role of collagen degradation in lymphoma invasion. From there, we can determine whether or not collagen degradation is required for lymphoma invasion , investigate the role of Rho GTPases, and more closely define key elements of cytoskeletal signaling that control invasion of drug-resistant lymphoma.

REFERENCES

[1] A. Mass. Hodgkin, Thomas (1798-1866,) physician and social reformer. Oxford Press, Oxford Dictionary of National Biography, (2004).

[2] W.C. Chan, J.O. Armitage, R. Gascoyne, A clinical evaluation of the International Lymphoma Study Group classification of non-Hodgkin's lymphoma, Blood 89 (1997) 3909-3918.

[3] M. Jordan, L. Wilson, Microtubules and actin filaments: dynamic targets for cancer chemotherapy, Current Opinion in Cell Biology 10 (1998) 123-130.

[4] A. Fojo, K. Ueda, D. Slamon, D. Poplack, M. Gottesman, I. Pastan, Expression of a multidrug-resistant gene in human tumors and tissues, Proceedings of the National Academy of Science of the United States of America 84 (1987) 265-269.

[5] R. Fisher, E. Gaynor, S. Dahlberg, M. Oken, T. Grogan, E. Mize, J. Glick, C. Coltman, T. Miller, Comparison of a standard regimen (CHOP) with three intensive chemotherapy regimens for advanced non-Hodgkin's lymphoma, The New England Journal of Medicine 328 (1993)1002–10066.

[6] J. Vose, B. Link, M. Grossbard, M. Czuczman, A. Grillo-Lopez, P. Gilman, A. Lowe, L. Kunkel, R. Fisher, Phase II study of rituximab in combination with CHOP chemotherapy in patients with previously untreated, aggressive non-Hodgkin’s lymphoma, Journal of Clinical Oncology 19 (2001) 389-397.

[7] R. Mohammad, N. Wall, J. Dutcher, A. Al-Katib, The addition of bryostatin 1 to cyclophosphamide, doxorubicin, vincristine, and prednisone (CHOP) chemotherapy improves response in a CHOP-resistant human diffuse large cell lymphoma xenograft model, Clinical Cancer Research 6 (2000) 4950-4956.

[8] Y. Zheng, Y. Kong, E. Goetzl, Lysophosphatidic acid receptor-selective effects on Jurkat T cell migration through a matrigel model basement membrane, The Journal of Immunology 166 (2001) 2317-2322.

[9] S. Spiegal, S. Milstein, Sphingosine-1-phosphate: signaling inside and out, Federation of European Biochemical Societies Letters 476 (2000) 55-57.

[10] S. Spiegal, S. Milstein, Sphingosine-1-phosphate: an enigmatic signaling lipid, Nature Reviews Molecular Cell Biology 4 (2003) 397-407.

[11] G. Bergers, L. Benjamin, Angiogenesis: Tumorigenesis and the angiogenic switch, Nature Reviews Cancer 3 (2003) 401-410.

[12] E. Rungger-Brandle, G. Gabbiani, The role of cytoskeletal and cytocontractile elements in pathological processes, The American Journal of Physiology 110 (1983) 361-392.

[13] S. Su, K. Bayless, Molecular profile of endothelial invasion of three-dimensional collagen matrices: insights into angiogenic sprout induction in wound healing, The American Journal of Physiology 64 (2008) 1215-1229.

[14] V.S. Sethi, D.V. Jackson, D.R. White, Pharmacokinetics of vincristine sulfate in adult cancer patients, Cancer Research 41 (1981) 3551-3555.

[15] J.A. Leighton, M.K. Bay, A.L. Maldonado, Colchicine clearance is impaired in alcoholic cirrhosis, Hepatology, 14 (1991)1013-1015.

[16] E.K. Rowinsky, M. Jiroutek, P. Bonomi, Paclitaxel steady-state plasma concentration as a determinant of disease outcome and toxicity in lung cancer patients treated with paclitaxel and cisplatin, Clinical Cancer Research 5 (1999) 767-774.

[17] S.A. Maxwell, Z. Li, D. Jaya, S. Ballard, J. Ferrell, H. Fu, 14-3-3zeta mediates resistance of diffuse large B cell lymphoma to an anthracycline-based chemotherapeutic regimen, Journal of Biological Chemistry 284 (2009) 22379-22389.

[18] T. Mosmann, Rapid colorimteric assay for cellular growth and survival: application to proliferation and cytotoxicity assays, Journal of Immunological Methods 65 (1983) 55-63.

[19] J.G. Cory, J.A. Barltrop, T.C. Owen, Use of an aqueous soluble tetrazolium formazan assay for cell-growth assays in culture, Cancer Communications 3 (1991) 207-212.

[20] S.L. Voytik-Harbin, A.O. Brightman, B. Waisner, C.H. Lamar, S.F. Badylak, Application and evaluation of the Alamarblue assay for cell growth and survival of fibroblasts, In Vitro Cellular & Developmental Biology Animal 34 (1998) 239-246.

[21] A. ALahari, X. Trivelli, Y. Guérardel, L.G. Dover, G.S. Besra, J.C. Sacchettini, R.Reynolds, G.D. Coxon, L. Kremer, Thiacetazone, an antitubercular drug that inhibits cyclopropanation of cell wall mycolic acids in mycobacteria, PLoS ONE 2 (2007) e1343.

[22] B. Vasir, P. Reitz, G. Xu, A. Sharma, S. Bonner-Weir, G.C. Weir, Effects of diabetes and hypoxia on gene markers of angiogenesis in cultured and transplanted rat islets, Diabetologia 43 (200) 763-772.

[23] E.W. Thompson, S. Paik, N. Brunner, C.L. Sommers, G. Zugmaier, R. Clarke, Association of increased basement membrane invasiveness with absence of estrogen receptor and expression of vimentin in human breast cancer cell lines, Journal of Cellular Physiology 150 (2005) 534-544.

[24] C.L. Sommers, S.E. Heckford, J.M. Skerker, P. Worland, J.A. Torri, E.W. Thompson, S.W. Byers, Loss of epithelial markers and acquisition of vimentin expression in adriamycin- and vinblastine-resistant human breast cancer cell ines, Cancer Research 52 (1992) 5190-5197.

[25] S.H. Lang, C. Hyde, I.N. Reid, I.S. Hitchcock, C.A. Hart, A.A. Gordon-Bryden, J.M. Villette, M.J. Stower, N.J. Maitland, Enhanced expression of vimentin in motile prostate cell lines and in poorly differentiated and metastatic prostate carcinoma, The Prostate 52 (2002) 253-263.

[26] M. Gonzaels, B. Weksler, D. Tsuruta, R.D. Goldman, K.J. Yoon, S.B. Hopkinson, F.W. Flitney, J.C. Jones, Structure and function of a vimentin-associated matrix adhesion in endothelial cells, Molecular Biology of the Cell 12 (2001) 85-100.

[27] M. Yoon, R.D. Moir, V. Prahlad, R.D. Goldman, Motile properties of vimentin intermediate filiament networks in living cells, Journal of Cell Biology 143 (1998) 147-157.

[28] V. Prahlad, M. Yoon, R.D. Moir, R.D. Vale, R.D. Goldman, Rapid movement of vimentin on microtubule tracks: kinesin-dependent assembly of intermediate filament networks, Journal of Cell Biology 143 (1998) 159-170.

[29] H.U. Keller, A. Naef, A. Zimmermann, Effects of colchicines, vinblastine and nocodazole on polarity, motility, chemotaxis, and cAMP levels of human polymorphonuclear leukocytes, Experimental Cell Research 153 (1984) 173-185.

[30] R. Samarakoon, C.E. Higgins, S.P. Higgins, P.J. Higgins, Differential requirement for MEK/ERK and SMAD signaling in PAI-1 and CTGF expression in response to microtubule disruption, Cellular Signaling 21 (2009) 986-995.

[31] Y. Zhao, Z. Zong, H. Xu, RhoC expression level is correlated with the clinicopathological characteristics of ovarian cancer and the expression levels of ROCK-I, VEGF, and MMP9, Gynecologic Oncology 116 (2010) 563-571.

[32] A.C. Kimmelman, A.F. Hezel, A.J. Aguirre, H. Zheng, J. Paik, Genomic alterations link Rho family of GTPases to the highly invasive phenotype of pancreas cancer, PNAS 105 (2008) 19372-19377.

[33] J. Shao, H. Wang, L. Yang, X. Deng, Effects of Rho proteins on the cytoskeletal activity and the growth regulation in tumor cells, Journal of Biomedical Engineering 25 (2008) 1462-1465.

[34] R. Gupta, Cross-resistance of nocodazole-resistant mutants of CHO cells toward other microtubule inhibitors: similar mode of action of benzimidazole carbamate derivateives and NSC 181928 and TN-16, Molecular Pharmacology 30 (1986) 142-148.

[35] H. Yamaguchi, J. Condeelis, Regulation of the actin cytoskeleton in cancer cell migration and invasion, Biochimica et Biophysica Acta- Molecular Cell Research 1773 (2006) 642-652.

[36] A.M. Weaver, Invadopodia: specialized cell structures for cancer invasion, Clinical and Experimental Metastasis 23 (2006) 97-105.

[37] D. Wang, Z. Zhao, A. Caperell-Grant, G. Yang, S. Mok, J. Liu, R. Bigsby, Y. Xu, S1P differentially regulates migration of human ovarian cancer and human ovarian surface epithelial cells, Molecular Cancer Therapy (2008) 1993-2002.

[38] T. Yamada, K. Sato, M. Komachi, E. Malchinkhuu, M. Tobo, T. Kimura, A. Kuwabar, Y. Yanagita, Lysophosphatidic acid (LPA) in malignant ascites stimulates motility of human pancreatic cancer cells through LPA1, Journal of Biological Chemistry 279 (2004) 6595-6605.

[39] H. Li, Lysophosphatidic acid stimulates cell migration, invasion, and colony formation as well as tumorigenesis/metastasis of mouse ovarian cancer in immunocompetant mice, Molecular Cancer Therapeutics 8 (2009) 1692-1701.

[40] A. Boucharaba, C.M. Serre, J. Guglielmi, J.C. Bordet, P. Clézardin, O. Peyruchaud, The type 1 lysophosphatidic acid receptor is a target for therapy in bone metastases, Proceedings of the National Academy of Sciences of the United States of America 103 (2006) 9643-9648.

[41] S. Sengupta, K.S. Kim, M.P. Berk, R. Oates, P. Escobar, Lysophosphatidic acid downregulates tissue inhibitor of metalloproteinases, which are negatively involved in lysophosphatidic acid-induced cell invasion, Oncogene 26 (2007) 2894-2901.

[42] C.I. Lin, C.N. Chen, M.T. Huang, S.J. Lee, C.H. Lin, C.C. Chang, H. Lee, Lysophosphatidic acid up-regulates vascular endothelial growth factor-C and lymphatic marker expressions in human endothelial cells, Cellular and Molecular Life Sciences 65 (2008) 2740-2751.

[43]K.J. Bayless, G.E. Davis, Sphingosine-1-phosphate markedly induces matrix metalloproteinase and integrins-dependent human endothelial cell invasion and lumen formation in three-dimensional collagen and fibrin matrices, Biochemical and Biophysical Research Communications 312 (2003) 903-913.

[44] S. Linder, The matrix corroded: podosomes and invadopodia in extracellular matrix degradation, Trends in Cell Biology 17 (2007) 107-117.

[45] P. De Bruyn, Theories of Amoeboid movement, The Quarterly Review of Biology 22 (1947) 1-24.

[46] F. Sabeh, R. Shimizu-Hirota, S.J. Weiss, Protease-dependent versus –independent cancer cell invasion programs: three-dimensional amoeboid movement revisited, Journal of Cell Biology 185 (2009) 11-19.

[47] K.E. Fisher, A. Pop, W. Koh, N.J. Anthis, W.B. Saunders, Tumor cell invasion of collagen matrices requires coordinate lipid agonist-induced G-protein and membrane-type matrix metalloproteinase-1-dependent signaling, Molecular Cancer 5:69 (2006) 1-23.

CONTACT INFORMATION

Name:	Evan Michael Cherry
Professional Address:	c/o Dr. Kayla Bayless Department of Molecular & Cellular Medicine Reynolds Building Rm 442 Texas A&M University College Station, TX 77843
Email Address:	evianc1@neo.tamu.edu
Education:	B.S., Chemical Engineering, Texas A&M University, May 2010 Summa Cum Laude Undergraduate Research Scholar Honors Undergraduate Research Fellow Phi Kappa Phi Tau Beta Pi